RSC Advances

ROYAL SOCIETY OF CHEMISTRY

www.rsc.org/advances

Mesoporous silicas: improving the adsorption efficiency of phenolic compounds by the removal of the amino group from functionalized silicas

Amine Morsli[a], Abdellah Benhamou[a,b], Jean-Philippe Basly[b*], Michel Baudu[b], Zoubir Derriche[a]

[a]*Université des Sciences et Technologie d'Oran "M. Boudiaf", Laboratoire d'Ingénierie des Procédés de l'Environnement, B.P. 1505, Oran El M'Nouer, Algeria.*

[b]*Université de Limoges, EA 4330 Groupement de Recherche Eau Sol Environnement, 123 Avenue Albert Thomas, Limoges, 87060 Cedex, France.*

* Corresponding author

J.P. Basly

Université de Limoges, EA 4330 Groupement de Recherche Eau Sol Environnement

123 Avenue Albert Thomas

87060 Limoges

France.

Abstract

In this study, dimethyloctylamine functionalized-mesoporous silicas (MCM-41 and MCM-48 samples), designed for anionic and cationic species sorbents, have been successfully desaminated by ethanolic extraction to lead to materials able to remove, from aqueous effluents, neutral phenolic polluants, 4-nitrophenol and 2,4,6-trichlorophenol. Solvent extraction was further applied to amine-functionalized MCM-41 and MCM-48 mesoporous materials with different chain length (N,N-dimethyldodecylamine, dodecylamine and hexadecylamine). The hexagonal mesoporous structure of MCM-41 and the three-dimensional cubic mesoporous structure of MCM-48 remain intact after dimethyloctylamine amination and template removal. N_2 adsorption-desorption isotherms of the different mesoporous materials are of type IV according to the IUPAC classification. Alcoolic extraction of the dimethyloctylamine moiety leads to materials with a wide open pore structure particularly suitable for fast adsorption of hydrophobic molecules. Isotherm data at ambient temperature were well fitted with the Langmuir model. Solvent extraction was further applied to amine-functionalized MCM-41 and MCM-48 mesoporous materials with different chain length (N,N-dimethyldodecylamine, dodecylamine and hexadecylamine) and a statistical analysis of the sorption capacities vs. structural properties was performed. ANOVA Kruskal-Wallis tests showed that pollutant adsorption was not dependent of the type of mesoporous silicas (MCM-41 vs. MCM-48) while pollutant adsorption was dependent of the phenolic structure (PNP vs. TCP). A (weak linear) correlation between the pore size and sorption capacities could be established.

Keywords: amino-functionalized mesoporous silicas, MCM-41, MCM-48, template extraction, calcination, phenols, sorption.

1. Introduction

The application of mesoporous silicas in adsorption and catalysis studies is currently the object of an extensive research since last decades.[1-5] These materials are characterized by high surface areas, uniform and controllable pore sizes and the periodic order of their pore packing. Functionalization of the pore channels provide new opportunities for fine-tuning the properties of these materials and amines are one of the most prominent chemical functionalities in this field.[4]

Adsorption of ionic species (both cationic and anionic)[4, 6-13] have been demonstrated with excellent sentivities and high capacities using aminated-functionalized mesoporous silicas with wide hydrophilic channels. Unfortunately, adsorption of organic (uncharged) compounds is disavantaged. In this case, to enhance the adsorption of organic pollutants, Sayari[14] suggested the removal of the amine template to create hydrophobic surfaces and open-pore structures. Calcination[15,16] oxidation[17-20] or solvent extraction.[14, 15, 21-23] have been suggested for their efficiency.

The focus of the present study was the template removal, by alcoholic extraction or calcination, from dimethyloctylamine-MCM-41 and dimethyloctylamine-MCM-48, two ordered mesoporous silicas from the Mobil M41S family of materials.[24-26] Solvent extraction was further applied to amine-functionalized MCM-41 and MCM-48 mesoporous materials with different chain lengths (N,N-dimethyldodecylamine, dodecylamine and hexadecylamine) [10, 11]. Phenol and its derivatives are considered as priority and hazardous pollutants because of their high toxicity, carcinogenicity and resistance to biodegradation and are widely used as reflected by their inclusion in the list of high volume production chemicals.[27] The different mesoporous materials were evaluated toward the removal of p-nitrophenol (PNP) and 2,4,6-trichlorophenol (TCP), chosen as phenolic compounds.

2. Experimental procedures

2.1. Materials and synthesis

All chemicals used in the experiments were purchased as analytical purity or highest purity available and used without any further treatment. MCM-41 and MCM-48 mesoporous silicas were, according to previous methods,[10, 11, 28, 29] prepared using Cetyltrimethylammonium Bromide, fumed silica for MCM-41 and TEOS for MCM-48. The solutions were hydrothermally treated and the solids were dried in air. The functionalization was achieved through post-synthesis. Mesoporous silicas (5 g) were added to an emulsion of N-N dimethyloctylamine (7 g) in distilled water (78 g) under magnetic stirring (30 min) and the mixture was sealed and heated in a Teflon autoclave for 72 h at 25°C . The product was recovered

by vacuum filtration, washed several times with Milli-Q water, and dried to lead to materials A (DMOA-41A and DMOA-48A). Solvent extraction was based on the work of Sayari[14] and used ethanol as extracting solvent. The experiments were carried out in a soxhlet apparatus and lead to Materials B (Table 1). Materials C were obtained by calcination at 550°C during 6 hours.

2.2. Characterization

Thermogravimetric curves were carried out on a TGA 2950 high-resolution thermogravimetric analyzer NETZSCH Iris TG 209C. The FTIR spectra were recorded on a Bruker Vector 22 FTIR spectrometer in the region 4000–400 cm^{-1} using the KBr method. Nitrogen physisorption was measured using a Micromeritics ASAP 2000 and ASAP 2010 at 77K. The specific surface areas were calculated from the Brunauer-Emmett-Teller (BET) equation and the pore size distribution using the Barett-Joyner-Halenda method by analysis of the desorption branch. The small-angle X-ray diffraction (XRD) patterns of the samples were collected with a Brucker AXS D-8 X-ray powder diffractometer using Cu Kα radiation (λ = 1.5418 Å). Zeta potential measurements were conducted in triplicate using a Zetaphoremeter IV (CAD instruments).

2.3. Adsorption studies

Stock solutions of nitrophenol (Sigma-Aldrich, 1000 $mg.L^{-1}$) and 2,4,6-trichlorophenol (Sigma-Aldrich, 750 $mg.L^{-1}$) were prepared in Milli-Q water. Adsorption kinetics and isotherms were performed at least in triplicate on an orbital shaker (200 rpm). Sorbent (100 mg) was thoroughly mixed with various concentrations of phenolic compounds (from 10 to 1000 mg/L for 4-NP and from 10 to 750 mg/L for 2,4,6 TCP) to a final volume of 100 mL. The samples were filtered with a syringe filter (0.20µm). Trichlorophenol (pK_a=6.21) and nitrophenol (pK_a=7.15) concentrations were determined using a Varian Cary UV 50 Probe spectrophotometer at 286 and 318 nm respectively. Experimental curves were fitted using non-linear regression method and Statistica 6.0 software; their suitability was assessed on the basis of R^2.

3. Results and Discussion

3.1. Dimethyloctylamine mesoporous silicas: characterization, ethanolic extraction vs. calcination.

FTIR peaks at 2925 and 2855 cm^{-1} were attributed to the CH_2 stretching vibrations originating from the amino template (Figure 1A). These peaks disappeared after calcination and less than 10% of DMOA (estimated by Thin Layer Chromatography) were observed after ethanolic treatment. Further analyses

were conducting using thermogravimetric analyses (Figure 1B). Three major mass losses vs. temperature were observed (Table 2). A first loss between 25°C and 150°C is assigned to adsorbed water and solvent molecules. The template loss starts at nearly 150°C and occur in several steps, which may related to different interactions between the organic template. Above 600°C, samples exhibit a weight loss due to the deshydroxylation of the silicate networks.

X-ray diffraction patterns of the mesoporous materials were compared. In the pattern of MCM-41, a dominant (100) peak reflection is attributed to the 2D-hexagonal symmetry *(p6mm).*[24] Dimethyloctylamine grafting to MCM-41 caused a considerable decrease in the XRD intensity. The peaks (211), (220), (321), (420) and (332) were associated with *Ia3d* cubic symmetry in the pattern of MCM-48 (Figure 1C). The highly mesostructure of the MCM-41 and MCM-48 mesoporous silicas was not affected by the treatment. XRD patterns show several scattering peaks in the low 2-theta region corresponding to <100> and <211> Bragg reflections for MCM-41 and MCM-48 further confirming that the hexagonal mesoporous structure of MCM-41 and the three-dimensional cubic mesoporous structure of MCM-48 remain intact after amination and template removal. A shift of the unit cell parameter was observed after solvent-template removal while this parameter decreased after calcination for MCM-41. In contrast, a_0 increased with calcination and decreased with solvent-extraction for MCM-48. N_2 adsorption-desorption isotherms of the mesoporous materials are of type IV according to the IUPAC classification. In accordance with the above XRD patterns presented above, isotherm curves were similar after modifications of the MCM-41 and MCM-48 mesoporous silicas. Structural and textural parameters are summarized in Table 3. The nonexpanded calcined (MCM-41) parent sample exhibited a reversible adsorption-desorption isotherm with the characteristic nitrogen condensation evaporation step at a relative pressure of 0.3 and exhibits a H1 hysteresis loop, characteristic of periodic mesoporous materials. [24, 25] Low pore volume and surface areas and broad PSD were observed for aminated materials (DMOA-41A and 48A) containing both CTMA and DMOA surfactants. Alcoolic extraction of the amine moiety (DMOA-41B and 48B) which contained about 50 wt % of cetyltrimethylammonium (CTMA) surfactant leads to materials with a wide open pore structure particularly suitable for fast adsorption of hydrophobic molecules. As expected, calcined material (DMOA-41C and 48C) exhibited highly enlarged pores with relatively narrow size distribution. It is well-known that functionalization decreases the surface area and pore volume since the terminal organic groups are tethered inside the pores of the mesoporous silicas. The removal of the template by both

ethanolic extraction (materials B) and calcination (materials C) sharply increased the surface area and pore volume.

Furthermore, the average pore volume observed for MCM-48 materials are slightly lower than that of MCM-41 materials. Ethanolic extraction and/or calcination modified the surface charge properties of materials. Isolectric points (IEP) shifted to higher values after amination which provided an indirect evidence of the existence of cationic groups in the structure. IEP point decreased with ethanolic extraction and calcination (Table 4). It has been suggested that the removal of the template by solvent-extraction better preserves the crystallinity and pore structure of the material and calcination increases the condensation degree of the silica and leads to a shrinkage of the MCM framework.[30]

3.2. Adsorption of p-nitrophenol and 2,4,6-trichlorophenol

Ethanolic extraction of the DMOA amine moiety significantly improved the sorption capacities (Table 5) toward phenolic compounds while calcination leads to weak sorption properties. More than 70% of the phenols were removed by Materials B (conditions are given in Table 5) while less than 30% of heavy metals were removed by Materials B in the same conditions (these last results could be compared with previous publications [10,11] on (aminated) mesoporous silicas). Materials C obtained by calcination were consequently not further studied for the adsorption of phenolic polluants . Inumaru [31-33] suggested that both hydrophilic and hydrophobic groups of adsorbates interacted with hydroxyl groups and organic moieties on the pore surface of organic–inorganic silica, respectively. Phenolic compounds have both hydrophobic phenyl groups and hydrophilic hydroxyl groups. Materials B after ethanolic extraction have hydrophobic methyl groups and hydrophilic hydroxyl; and phenolic compounds are expected to have two types of adsorbent–adsorbate interactions. One interaction is hydrogen-bonding between hydrophilic hydroxyl groups of MCM-41 and MCM-48B and adsorbates. The other one is $\pi-\pi$ interaction between benzene rings and organic moieties of MCM-41B and MCM-48B. The initial amount of adsorbed 4-NP or 2,4,6-TCP increased gradually up to 50 min and slowly reached the maximum concentration within 60 min. Pseudo-second order model (equation 1) fits well with the kinetic data obtained for Material B (Table 6) while first-order model failed to reproduce the data.

$$q = \frac{k_2 t q_e^{\,2}}{1 + k_2 t q_e} \qquad (1)$$

The possibility of intraparticle diffusion (Table 6) was explored by Weber-Morris intraparticle diffusion model (equation 2)

$$q_t = k_d t^{1/2} + L \qquad (2)$$

where k_d (mg g^{-1} $min^{-0.5}$) is the intraparticle diffusion rate constant and L is the intercept representative of the boundary layer thickness. The first sharp portion of the Weber-Morris plots (not shown) indicates that the sorption of NP and TCP is controlled by external mass transfer and the plots do not pass through the origin and have intercepts (Table 6) characteristics of the boundary layer thickness.

The equilibrium adsorption isotherm is the basic requirement in the design of adsorption systems. Isotherm data at ambient temperature (Figure 2) for DMOA-41B and DMOA-48B were well fitted with the Langmuir model (equation 3) based on assumptions that monolayer coverage of adsorbate occurs over homogeneous sites and a saturation point is reached where no further adsorption can act.

$$q_e = q_{max} \frac{k_L C_e}{1 + k_L C_e} \qquad (3)$$

Where q_e is the adsorption capacity of the adsorbent (mg/g); C_e is the equilibrium concentration of adsorbate in solution (mg/L); q_{max} is the maximum monolayer adsorption capacity (mg/g); k_L is the adsorption equilibrium constant related to the affinity of the binding sites and energy of adsorption (L/mg). Table 7 summarizes the results.

Solvent extraction was further applied to amine-functionalized MCM-41 and MCM-48 mesoporous materials with different chain length (N,N-dimethyldodecylamine, dodecylamine and hexadecylamine). Figure 2 shows 4- NP and 2, 4, 6 -TCP adsorption isotherms on Materials B. The adsorption closely follows a Langmuir isotherm (figure 2) in accordance with the results obtained for dimethyloctylamine mesoporous silicas and the Langmuir parameters are given in Table 7. The sorption performance of the Materials B was compared to other sorbents [34-51] (Table 7).

A statistical analysis of the sorption capacities (Table 7) vs. textural and structural properties of materials B (Table 3 and 4) was performed. The normality of variables distribution was checked by applying the Shapiro-Wilk statistical test and in all cases, the distribution was far from normal. Non-parametric tests were applied and ANOVA Kruskal-Wallis tests showed that pollutant adsorption was not dependent of the type of mesoporous silicas (MCM-41 vs. MCM-48) (Figure 4A); in contrast,

pollutant adsorption was dependent of the phenolic structure (PNP vs. TCP- Figure 4B). Data were analysed using the factor analysis (Figure 4C) in order to highlight the relation between the elements. Only the factors loading greater than 0.7 were considered important. The two factors describe 69% of the total variability contained in the raw data set. The eigen values are 2.29 (F1) and 1.82 (F2) and statistical estimate revealed a (weak) correlation between the pore size and q_{max} (F1). Plotting q_{max} vs. pore size (Figure 4D) confirms the weak relationship and a linear function could be established.

Conclusion

The experimental analysis indicate that the removal of the amine moiety by ethanolic extraction from aminated-mesoporous silicas leads to materials able to remove phenolic polluants, 4-nitrophenol and 2,4,6-trichlorophenol in this study, from aqueous media. Calcination of aminated-mesoporous silicas failed the improve the sorption capacities. From present and previous results, it could be interesting in the future to evaluate the partial removal of the amine moiety from modified mesoporous silicas which could offer the simultaneous removal of charged (both cationic and anionic) and neutral organic pollutants from aqueous media.

Acknowledgments

A. Benhamou gratefully acknowledges support from collaborative Project No. 87/ENS/FR/2007-2009 between Limoges University and Oran Science and Technology University.

References

1 A. Sayari and S. Hamoudi, *Chem. Mater*., 2001, **13**, 3151-3168.

2 M. Hartmann, *Chem. Mater.*, 2005, **17**, 4577-4593.

3 F.Hoffmann, M. Cornelius, J. Morell and M. Fröba, *Angew. Chem. Int. Ed*., 2006, **45**, 3216-3251.

4 T. Yokoi, Y. Kubota and T. Tatsumi, *Appl. Catal. A-Gen*., 2012, **451**, 14-37.

5 S.H. Wu, C-Y. Mou, H-P. Lin and *Chem. Soc. Rev.,* 2013, **42**, 3862-3875.

6 H. Yoshitake, T. Yokoi and T. Tatsumi, *Chem. Mater.*, 2002 **14**, 4603-4610.

7 H. Yoshitake, T. Yokoi and T. Tatsumi, *Chem. Mater.,* 2003, **15**, 1713-1721.

8 H. Yoshitake, E. Koiso, H. Horie and H. Yoshimura, *Micropor. Mesopor. Mater.*, 2005, **85**, 183-194.

9 J. Aguado, J.M. Arsuaga, A. Arencibia, M. Lindo and V. Gascon, *J. Hazard. Mater.,* 2009, **163**, 213-221.

10 A. Benhamou, M. Baudu, Z. Derriche and J.P. Basly, *J. Hazard. Mater*., 2009, **171**, 1001-1008.

11 A. Benhamou, J.P. Basly, M. Baudu, Z. Derriche and R. Hamacha, *J. Colloid Interf. Sci.*, 2013, **404**, 135-139.

12 L.F. Koong, K.F. Lam, J. Barford, G. MacKay and *J. Colloid Interf. Sci.,* 2013, **395**,230-240.

13 I. Sierra and D. Perez-Quintanilla, *Chem. Soc. Rev.*, 2013, **42**, 3792-3807.

14 A. Sayari, S. Hamoudi and Y. Yang, *Chem. Mater,.* 2005, **17**, 212-216.

15 P.T. Tanev and T.J. Pinnavaia, *Chem. Mater.,* 1996, **8**, 2069-2079.

16 R. Kumar, H.T. Chen, J.L.V. Escoto, V.S.Y. Lin and M. Pruski, *Chem. Mater.,* 2006, **18**, 4319-4327.

17 E. Meretei, J. Halász, D. Meshn, Z. Kónya, T.I. Korányi, J.B. Nagy and I. Kiricsi, *J. Mol. Struct*., 2003, **651-653**, 323-330.

18 S. Hitz and R. Prins, *J. Catal.,* 1997, **168**, 194-206.

19 J. Kecht and T. Bein, *Micropor. Mesopor. Mat.,* 2008, **116**, 123-130.

20 J. Goworek, A. Kierys and R. Kusak, *Micropor. Mesopor. Mat.,* 2007, **98**, 242-248.

21 M. Nassi, E. Sarti, L. Pasti, A . Martucci, N. Marchetti, A. Cavazzini, F. Di Renzo and A. Galarneau, *J. Porous Mater.* 2014, **21**, 423-432.

22 W.A. Gomes Jr., L.A.M. Carsodo, A.R.E. Gonzaga, L.G. Aguiar and H.M.C. Andrade, *Mater. Chem. Phys.*, 2005, **93**, 133-137.

23 H. Ji, Y. Fan, W. Jin, C. Chen and N. Xu, *J. Non-Cryst. Solids.*, 2008, **354**, 2010-2016.

24 J. S. Beck, J. C. Vartuli, W. J. Roth, M. E. Leonowicz, C. T. Kresge, K. D. Schmitt, C. T.W. C. T.W. Chu, D. H. Olson, E. W.Sheppard, S. B. McCullen, J. B. Higgins and J. L. Schlenker, *J. Am. Chem. Soc.*, 1992, **114**,10834-10843.

25 C.T. Kresge, M.E. Leonowicz, W.J. Roth, J.C. Vartuli and J.S. Beck, *Nature*, 1992, **359**, 710-712.

26 J. C. Vartuli, K. D. Schmitt, C. T. Kresge, W. J. Roth, M. E. Leonowicz, S. B. McCullen, S. D. Hellring, J. S. Beck and J. L. Schlenker, *Chem. Mater.,* 6 1994, **6**, 2317-2326.

27 OECD, 2008. The 2004 organisation for economic co-operation and development (OECD) list of high production volume chemicals .Available from: <http://www.oecd.org/dataoecd/55/38/33883530.pdf>.

28 A. Sayari and Y. Yang, *J. Phys. Chem. B*, 2000, **104**, 4835–4839.

29 S. Wang, D. Wu, Y. Sun and B. Zhong, *Mater. Res. Bull.* 2001, **36**, 1717–1720.

30 A. Jomekian, S.A.A. Mansoori, B. Bazoyaar and A. Moradian, *J. Porous Mater*., 2012, **19**, 979-988.

30 R. Vathyam, E. Wondimu, S. Das, C. Zhang, S. Hayes, Z. Tao and T. Asefa, *J. Phys. Chem. C,* 2011, **115**, 13135-13150.

31 K. Inumaru, Y. Inoue, S. Kakii, T. Nakano and S. Yamanaka, *Chem. Lett.,* 2003, **32**, 1110-1111.

32 K. Inumaru, Y. Inoue, S. Kakii, T. Nakano and S. Yamanaka, *Phys. Chem. Chem. Phys.,* 2004, **6**, 3133-3139.

33 K. Inumaru, T. Nakano and S. Yamanaka, *Micropor. Mesopor. Mater*., 2006, **95**, 279-285

34 B. Petrova, T. Budinova, B. Tsyntsarski, V. Kochkodan, Z. Shravro and N. Petrov, Chem. Eng. J., 2010, **165**, 258-264.

35 Q.S. Liu, T. Zheng, P. Wang and J.P. Jiang, N.Li, *Chem. Eng. J.,* 2010, **157**, 348-356.

36 B.C. Pan, W. Du, W. Zhang, X. Zhang, Q. Zhang, B. Pan and L. Lv, Q. Zhang, J. Chen, *Environ. Sci. Technol*., 2007, **41**, 5057-5062.

37 M. Ahmaruzzaman and D.K.Sharma, *J. Colloid Interf. Sci.*, 2005, **287**, 14-24.

38 E. Gonzalez-Serranoa, T. Corderoa, J. Rodriguez-Mirasola, L. Cotorueloa and J.J. Rodriguez, *Water Res*., 2004, **38**, 3043–3050**.**

39 A. Dabrowski, P. Podkoscielny and O.V.Marijuk, *Chemosphere*., 2005, **58**, 1049–1070.

40 I.A.W. Tan, A.L. Ahmad and B.H. Hameed, *J. Hazard. Mat*., 2009, **164**, 473–482.

41 Q. Zhoua, H.P. Hea, J.X. Zhua, W. Shen, R.L. Frost and P. Yuan, *J. Hazard. Mater.,* 2008, **154**, 1025-1032.

42. B. Zhanga, F. Li, T. Wub, D. Sunb and Y. Li, *Colloid Surf. A. Physicochem. Eng. Aspects*, 2015, **464**, 78-88.

43. C. Muniz-Lopez, J. Duconge and R. Roque-Malherbe, *J. Colloid Interf. Sci.,* 2009, **329**, 11-16.

44 M. Anbia and M. Lasghari, *Chem. Eng. J*., 2009,**168**, 555-560.

45 B.H. Hameed, *Colloid Surf. A. Physicochem. Eng. Aspects*, 2007, **307**, 45-52.

46. A. Ersoz, A. Denitzli, I. Sener, A. Atilir, S. Diltemiz and R. Say, *Sep. Purif. Technol*., 2004, *38*, 173-179

47 A. Denitzli, G. Ozkan and M. Ucar, *Sep. Purif. Technol.* 2001, **24**, 255-262.

48 Y. Ku and K.C. Lee, *J. Hazard. Mater*. 2000, **B80**, 59-68.

49 F.C. Wu and R.L. Tseng, *J. Colloid Interf. Sci.* 2006, **294**, 21-30.

50 B. Shah, R. Tailor and A. Shah, *Environ. Sci. Pollut. Res.* 2012, **19**, 1171-1186.

51 M.M. Motsa, J.M. Twala, T.A.M. Msagati and B.B. Mamba, *Water Air Soil Poll.* 2012, **223**, 1555-1559.

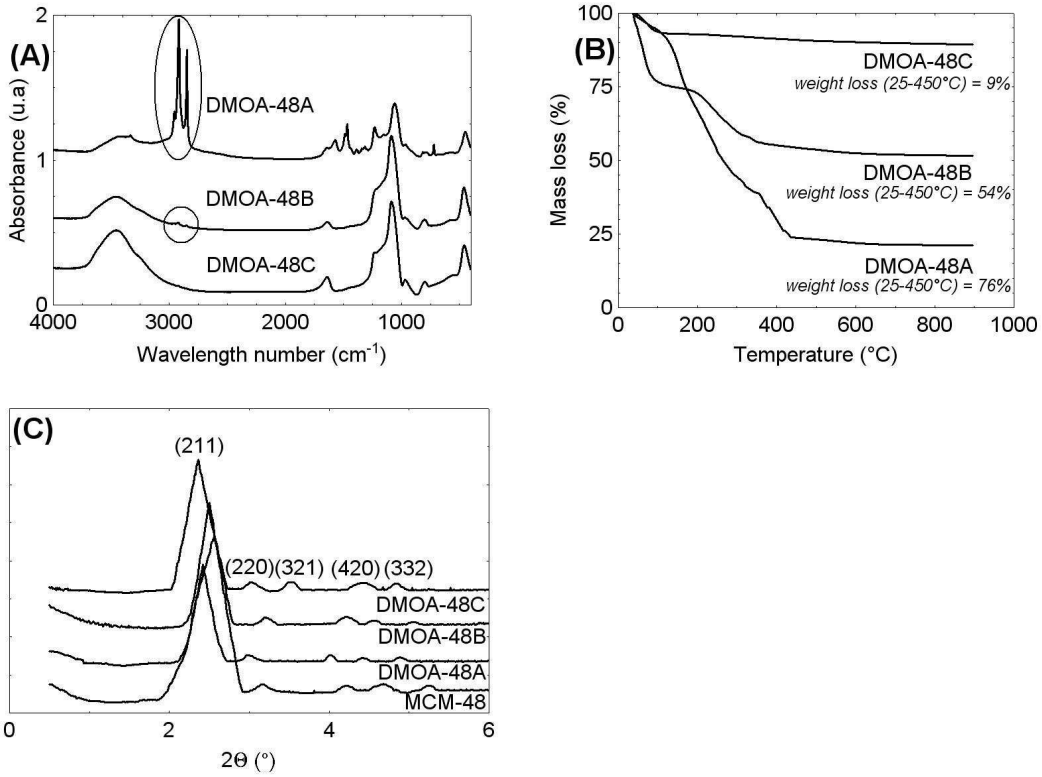

Figure 1. Dimethyloctylamine mesoporous MCM-48 silica (DMOA-48A), mesoporous silica obtained after DMOA-48A alcoolic extraction of the amine moiety (DMOA-48B) and calcined DMOA-48A (DMOA-48C). **(A)** FTIR spectra. Circles show the stretching vibrations originating from the amino template. **(B)** Thermogravimetric curves. **(C)** Low-angle XRD diffractograms.

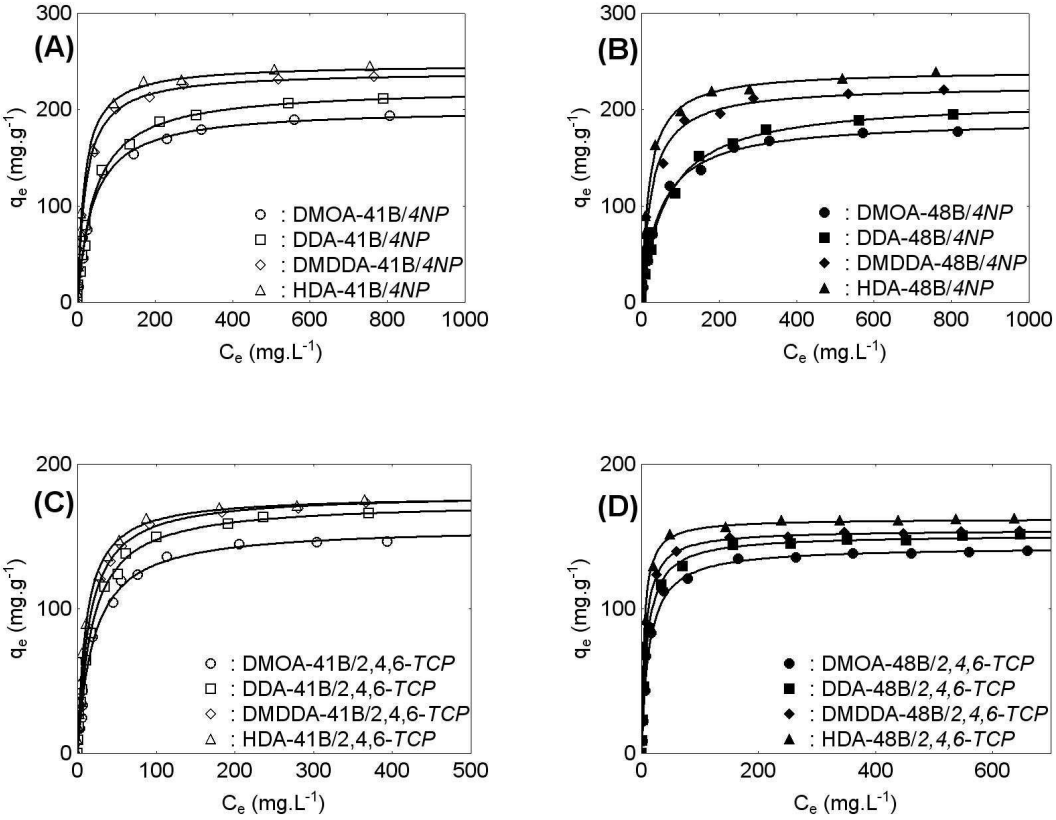

Figure. 2. Adsorption isotherms. The solid lines represent the fits with the Langmuir isotherms. [NP] = 10-1000 mg.L^{-1}, [TCP]= 10-750 mg.L^{-1}, $m_{sorbent}$= 100 mg, pH = 5.5 (TCP) and 6.0 (NP), ambient temperature, contact time= 24 hours, shaking rate= 200 rpm. Experimental points were obtained respectively from four replicates for 4-nitrophenol and three replicates for 2,4,6-trichlorophenol.

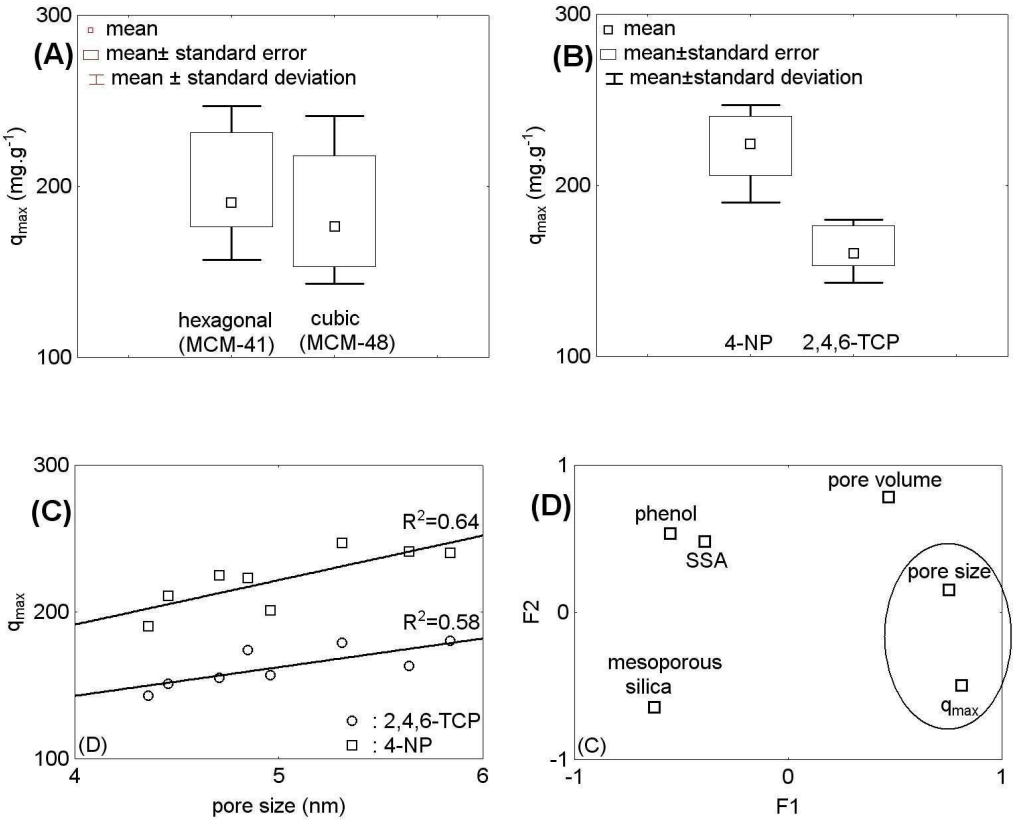

Figure 3. Statistical analysis of the sorption capacities vs. structural properties of the mesoporous silicas. **(A)** q_{max} vs. mesoporous silicas structure (p= 0.34, Z=0.94). **(B)** q_{max} vs. pollutant structure (p<0.01, Z=3.36). **(C)** q_{max} vs. pore size (n=16). **(D)** factor analysis (n=42, 6 variables).

Table 1. Mesoporous materials used in this study

Material	mesoporous silica	amine	treatment
MCM-41, MCM-48			
DMOA-41A	MCM-41	dimethyloctylamine	-
DMOA-41B	MCM-41	dimethyloctylamine	solvent extraction
DMOA-41C	MCM-41	dimethyloctylamine	calcination
DMOA-48A	MCM-48	dimethyloctylamine	-
DMOA-48B	MCM-48	dimethyloctylamine	solvent extraction
DMOA-48C	MCM-48	dimethyloctylamine	calcination
DMDDA-41B	MCM-41	dimethyldodecylamine	solvent extraction
DDA-41B	MCM-41	dodecylamine	solvent extraction
HDA-41B	MCM-41	hexadecylamine	solvent extraction
DMDDA-48B	MCM-48	dimethyldodecylamine	solvent extraction
DDA-48B	MCM-48	dodecylamine	solvent extraction
HDA-48B	MCM-48	hexadecylamine	solvent extraction

* The ending letter in the material name indicates : (A) aminated mesoporous silicas, (B) alcoolic extraction of the amine moieties, (C) calcination of the aminated mesoporous silica (A).

Table 2. Thermogravimetric curves- mass loss vs. temperature

Sample	Weight loss (%) 25-150°C	Weight loss (%) 150°- 450°C	Total weight loss (%)
DMOA-41A	12	64	76
DMOA-41B	25	21	46
DMOA-41C	7	3	10
DMOA-48A	17	59	76
DMOA-48B	25	29	54
DMOA-48C	7	2	9

Table 3 Textural and structural parameters

Material	Surface area ($m^2.g^{-1}$)	Pore size D_p (nm)	Pore volume ($cm^3.g^{-1}$)	2θ	$d_{(100)}$ (nm)	$d_{(211)}$ (nm)	a_0 (nm)
DMOA-41A	219	1.39	0.31	2.13	4.14	-	4.78
DMOA-41B	538	4.96	1.14	2.04	4.32	-	4.98
DMOA-41C	1284	9.66	1.59	2.19	4.05	-	4.67
DMOA-48A	176	1.28	0.23	2.42	-	3.65	8.94
DMOA-48B	458	4.36	0.91	2.50	-	3.53	8.64
DMOA-48C	1027	9.17	1.26	2.36	-	3.74	9.17
DDA-41B*	439	4.85	0.92				
DMDDA-41B*	373	5.84	0.97				
HDA-41B	284	5.31	0.98				
DDA-48B*	433	4.46	0.85				
DMDDA-48B*	381	4.71	0.82				
HDA-48B	316	5.64	0.93				

* From reference 10. The materials used in the adsorption studies are underlined.

Table 4 Isoelectric points*

	DMOA-41A	DMOA-41B	DMOA-41C	DDA-41B	DMDDA-41B	HDA-41B
pH_{iep}	8.5	5.3	3.7	3.9	3.8	5.1
	DMOA-48A	DMOA-48B	DMOA-48C	DDA-48B	DMDDA-48B	HDA-48B
pH_{iep}	9.1	4.3	3.5	4.5	3.9	4.9

*The mesoporous silicas are positively charged when $pH<pH_{iep}$ and negatively charged when $pH>pH_{iep}$. The materials used in the adsorption studies are underlined

Table 5 Sorption capacities

q_e ($mg.g^{-1}$)	MCM-41	DMOA-41A	DMOA-41B	DMOA-41C
PNP	48	41	83	31
TCP	33	25	70	19
q_e ($mg.g^{-1}$)	MCM-48	DMOA-48A	DMOA-48B	DMOA-48C
PNP	44	39	81	28
TCP	29	27	69	16

[PNP)] = [TCP] = 100 $mg.L^{-1}$, m= 100 mg, pH = 5.5 (TCP) and 6.0 (PNP), ambient temperature, contact time = 24 hours, shaking rate= 200 rpm.

Table 6 Kinetic parameters

		Second-order			Weber-Morris		
Material	Pollutant	k_2 ($g.mn^{-1}.mg^{-1}$)	q_e ($mg.g^{-1}$)	R^2	k_{id} ($mg.g^{-1}.mn^{-1/2}$)	L ($mg.g^{-1}$)	R^2
DMOA-41B	4-NP	$3.7.10^{-3}$	88	0.995	4.0	40	0.963
DMOA-48B		$1.5.10^{-3}$	82	0.998	3.0	28	0.948
DMOA-41B	2,4,6-TCP	$4..10^{-3}$	79	0.988	4.7	47	0.943
DMOA-48B		$1.2.10^{-3}$	74	0.991	3.9	35	0.951

Table 7 Langmuir parameters

4-NP	*DMOA-41B*	*DDA-41B*	*DMDDA-41B*	*HDA-41B*
q_{max} ($mg.g^{-1}$)	201±4	222± 5	240± 4	247± 5
k_L ($L.mg^{-1}$)	(2.55± 0.23)10^{-2}	(2.30± 0.20) 10^{-2}	(4.84± 0.42) 10^{-2}	(5.78± 0.57) 10^{-2}
R^2	0.992	0.994	0.994	0.992
	DMOA-48B	*DDA-48B*	*DMDDA-48B*	*HDA-48B*
q_{max} ($mg.g^{-1}$)	189± 4	210± 5	225± 5	241± 4
k_L ($L.mg^{-1}$)	(2.07± 0.16) 10^{-2}	(1.57± 0.13) 10^{-2}	(4.02± 0.38) 10^{-2}	(5.22± 0.36) 10^{-2}
R^2	0.994	0.994	0.992	0.996
	Carbonaceous materials	Modified clay	Zeolithe	Synthetic resins
q_{max} ($mg.g^{-1}$)	179 [34], 313 [35], 333 [36], 526 [37], 268 [42], 376-542 [49]	436 [41]	330 [43], 55-91 [50], 19 [51]	11-21 [46], 16 [47], 931 [48]
2,4,6-TCP	*DMOA-41B*	*DDA-41B*	*DMDDA-41B*	*HDA-41B*
q_{max} ($mg.g^{-1}$)	156± 3	174± 3	180± 3	179± 4
k_L ($L.mg^{-1}$)	(4.97± 0.39) 10^{-2}	(5.62± 0.33) 10^{-2}	(6.98± 0.40) 10^{-2}	(9.30± 0.82) 10^{-2}
R^2	0.992	0.996	0.996	0.991
	DMOA-48B	*DDA-48B*	*DMDDA-48B*	*HDA-48B*
q_{max} ($mg.g^{-1}$)	143± 2	151± 2	155± 3	162± 4
k_L ($L.mg^{-1}$)	(7.83± 0.70) 10^{-2}	(15.3± 1.46) 10^{-2}	(10.7± 1.02) 10^{-2}	162± 4
R^2	0.990	0.990	0.990	0.976
	Carbonaceous materials	Modified clay	Zeolithe	Other mesoporous silicas
q_{max} ($mg.g^{-1}$)	479 [35], 476 [38], 794 [39], 247 [40]	123 [45]	1.5 [51]	500 [44]